Gerringa, L.J.A.; Laan, P.; Arrigo, K.R.; van Dijken, G.L. & Alderkamp, A.-C. (2019). The organic complexation of iron in the Ross sea. *Marine Chemistry*, 215, 103672

The organic complexation of iron in the Ross Sea

L.J.A. Gerringa[1], P. Laan[1] , K.R. Arrigo[2], G.L. van Dijken[2], A.-C. Alderkamp[2,3]

1: Department of Ocean Systems, NIOZ Royal Netherlands Institute for Sea Research, and Utrecht University, Den Burg, The Netherlands

2: Department of Earth System Science, Stanford University, USA

3: Biology Department, Foothill College, 12345 El Monte Road, Los Altos Hills, USA

Abstract
The Ross Sea Polynya (RSP) has the highest primary production of Antarctic waters. Iron (Fe) is one of the most important growth limiting factors in the Southern Ocean. Dissolved iron (DFe)-binding organic ligands play an important ecological role because they increase the residence time of the scarce Fe. Therefore, we studied the DFe-binding organic ligands in the vicinity of the Ross Sea during a cruise between 20 December 2013 and 5 January 2014. The DFe-binding organic ligands were measured using Competing Ligand Exchange Cathodic Stripping Voltammetry (CLE-CSV) with TAC as competing ligand. The DFe-binding organic ligand concentrations always exceeded the DFe concentrations except in the bottom nepheloid layer of the RSP. No relationship was found between depth and DFe-binding organic ligand concentrations in the RSP indicating that these ligands are resistant to degradation and are probably exported by high salinity shelf water into the circumpolar current. DFe-binding organic ligand concentrations were highest in the RSP and the Antarctic Circumpolar Current (ACC) west of the Ross Sea, in association with seasonal phytoplankton blooms, although no correlation was found with parameters reflecting phytoplankton abundance or species. Phytoplankton sources and sinks of DFe-binding organic ligands are likely related to the seasonal progression of the bloom. In 39% of the samples, two DFe-binding organic ligand groups were distinguished based on the difference in binding strength. The distinction was especially clear in the RSP and in the ACC west of the RSP (54 and 77% of the samples, respectively) where blooms occurred and much less in the low biomass waters of the ACC east of the RSP and ice covered eastern part of the Ross Sea (15 and 10% of the samples, respectively). In these waters, other environmental factors, like sea ice melt, probably explain the absence of distinct relationships between primary production and ligand characteristics.

1. Introduction

On 28 October 2016 in Hobart, Australia, delegates from 24 countries and the European Union agreed to designate the Ross Sea in the Southern Ocean as the world's largest marine protected area. This decision illustrates the ecological importance of the Ross Sea at both the regional and global scale. Not only is primary production in the Ross Sea high, it is also a site of deep-water formation and both factors drive significant oceanic CO_2 drawdown (Arrigo et al., 2008a, Dunbar et al., 1998). Specifically, coastal polynyas (areas of open water surrounded by ice) are hot spots for energy and carbon transfer between the atmosphere and ocean (Smith and Barber, 2007; Arrigo et al., 2008b; Smith et al., 2014) with the phytoplankton production of the Ross Sea Polynya (RSP) being highest of the coastal Antarctic seas (Arrigo and Van Dijken, 2003; Arrigo et al., 2008a, Arrigo et al., 2015).

Marine primary production is controlled by nutrients supply and light. In Antarctic waters, the micronutrient iron (Fe) is known to be limiting in high (macro-)nutrient low chlorophyll (HNLC) regions (de Baar et al., 1990; Martin et al., 1990, 1994; Boyd et al., 2007 and references therein). Dissolved Fe (DFe) concentrations are low because of the low solubility of Fe in seawater due to high pH and oxygen content (Millero, 1998) and because of limited Fe sources. In the Ross Sea, DFe availability can limit primary production and influence phytoplankton community structure (Sedwick et al., 2000; Arrigo et al., 2003: Coale et al., 2005; Sedwick et al., 2011; Kustka et al., 2015a, b). Indeed, DFe can be very low in the upper mixed layer (0.02–0.08 nM in the upper 100 m; Gerringa et al., 2015a) even early in the season when the polynya is still forming (December 2013) due to "early season depletion of the winter reserve" (Sedwick et al., 2011). DFe concentrations have been observed to increase with depth near the seafloor (~500 m on average) of the Ross Sea shelf (Hayes and Davey, 1975; Gerringa et al., 2015a). Elevated DFe coincided with decreased transmission, indicative of a bottom nepheloid layer (BNL). Another possible source of Fe in the Ross Sea is upwelling of modified Circumpolar Deep Water (mCDW), as suggested elsewhere in the Antarctic region (Sherrell et al., 2015). However, a regional circulation model showed that the mCDW could not play a major role as a DFe source in the Ross Sea, which has been supported by the results from recent expeditions (Marsay et al., 2014; Gerringa et al., 2015a; McGillicuddy, et al., 2015). Hatta et al. (2017) also recently confirmed this conclusion, showing that DFe of the inflowing Circumpolar

Deep Water (CDW) is reduced during on-shelf mixing with Antarctic Surface Water (AASW), and concluding that the presence of mDCW causes a strong near bottom density gradient that hinders Fe supply from the sediment. Apart from local sources such as sea ice melt at the rims of the polynya and lateral transport from land, upward fluxes from the sediment are the most important sources of DFe to surface waters of the Ross Sea (Marsay et al., 2014; Gerringa et al., 2015a; Hatta et al., 2017).

The solubility of Fe is increased above the solubility product of Fe-(hydr)oxides by complexation with dissolved organic ligands (Liu and Millero, 2002; Gledhill and Van den Berg., 1994; Rue and Bruland, 1995). These dissolved organic ligands consist of a large group of mostly unidentified organic molecules that bind metals, in this case Fe. They can be characterized by their conditional binding strength and concentration, expressed as binding sites for Fe in nano-equivalents of M Fe (neq M Fe). The K′ (M^{-1}) is expressed as logK′, with respect to Fe′, where the prime in the former indicates the conditional nature of K and the prime in the latter that the concentration of inorganic Fe and not ionic Fe is used. The most common method to measure DFe-binding organic ligands is by Competing Ligand Exchange Cathodic Stripping Voltammetry (CLE-CSV). These ligands are found at average concentrations of 0.2-13 neq M Fe and binding strengths varying from logK′=10 to 13. (Gledhill and Buck, 2012). They increase the residence time of Fe and influence its bioavailability to phytoplankton (Gledhill and Van den Berg, 1994; Rue and Bruland, 1995; Timmermans et al., 2001; Visser et al., 2003; Rijkenberg et al., 2008; Gledhill and Buck, 2012; Gerringa et al., 2015b; Slagter et al., 2017; Buck et al., 2015).

The DFe-binding organic ligands are not yet well described and identified, and consist of a pool of different groups such as siderophores, humic substances, polysaccharides and hemes (Mawji et al., 2011; Laglera, et al., 2011; Hassler et al., 2011; Gledhill and Buck, 2012; Gledhill et al., 2015; Boiteau et al., 2016; Hassler et al., 2017). These groups differ in origin and probably also in binding characteristics. Siderophores are produced by heterotrophic bacteria, and production is probably stimulated by Fe limitation. They have a relatively high Fe-binding strength (logK′>12) but are found at relatively low concentrations (pM) in the open ocean (Butler, 2005; Mawji et al., 2011; Boiteau et al., 2016; Velasquez et al., 2016). Most humic substances have a terrestrial origin and are also part of chromophoric dissolved organic matter (CDOM) (Nelson and Siegel, 2013). Marine humic substances exist as well, but it is still under

debate whether these contribute to the DFe-binding organic ligand pool, since some studies found good correlations between CDOM measurements or fluorescence of humic-like substances and DFe-binding organic ligands (Tani et al., 2003; Kitayana et al., 2009; Nakayama et al., 2011), whereas others did not (Heller et al., 2013; Wanatabe et al., 2018). Considering only terrestrial humics as DFe-binding dissolved organic ligands, the highest concentrations (>10 neq M Fe) are present in coastal areas, where they can form the major fraction of the total organic ligand pool (Laglera et al., 2007 and 2011; Hioki et al., 2014; Bundy et al., 2015; Slagter et al., 2017; Dulaquais et al., 2018). The binding strength of humic substances is assumed to be relatively low (logK' <11, Gledhill and Buck, 2012; Bundy at al., 2014; 2015), but this might not always be the case. For example, Slagter et al. (2017) observed no decrease in logK′ (stable at 12) in relation to increasing concentrations of humic substances in the Arctic Ocean in the Transpolar Drift. Polysaccharides and exopolymeric substances (EPS) probably play a role as DFe-binding organic ligands (Hassler et al., 2011; 2017). According to Hassler et al. (2017), this group of ligands might become the most important contributor to the ligand pool in open ocean surface waters. Humic substances are assumed to be very resistant to degradation and are thought to be refractory organic substances with residence times of >1000 years, whereas the residence time of EPS and polysaccharides is short (hours-three years) (Repeta and Aluwihare, 2006; Hansell et al., 2009; 2012). The residence time of siderophores is still unknown. For the DFe-binding organic ligand pool as a whole, Gerringa et al. (2015b) calculated a residence time of 1000 years in the North Atlantic Deep Water of the Western Atlantic Ocean, 2.5 to 4 times longer than the residence time of DFe in the same water mass. Therefore, the concentration of DFe is determined by competition between the DFe-binding organic ligands, scavenging particles, and precipitation as oxides. Consequently, transport of DFe from its source in seawater is facilitated by the DFe-binding organic ligands (Sander and Koschinsky, 2011; Thuróczy et al., 2012; Klunder et al., 2012; Hawkes et al., 2013; Slagter et al., 2017; 2019). Although dissolved organic ligands are essential to keep Fe in solution and Fe availability limits phytoplankton growth in the Ross Sea, there is little available information on the DFe-binding organic ligands, with the exception of recently published data from a coastal area near Terra Nova Bay (Rivaro et al., 2018). They found high concentrations of both DFe (0.54-4.51 nM) and DFe-binding organic ligands, which enabled the accumulation of these high DFe concentrations. In this study, we present data on DFe-binding organic ligands in the Fe limited RSP (Alderkamp et al., in press)

obtained during a cruise on the RVIB *Nathaniel B. Palmer* from December 2013 to January 2014. The characteristics of the ligands, concentrations and binding strength, as well as whether a single or multiple different DFe-binding organic ligand groups could be distinguished, were evaluated with respect to concentrations of DFe and phytoplankton. These data were compared to data from adjacent ice covered waters in the eastern Ross Sea and to two areas in the Antarctic Circumpolar Current (ACC), east and west of the Ross Sea. Results from this research will improve the understanding of the Fe cycle in the RSP and via Ross Sea deep water formation also throughout the Fe-limited Southern Ocean.

2. Methods

2.1. Sampling

The cruise NBP13-10 of the RVIB *Nathaniel B. Palmer* took place from December 2013 to January 2014 (for full details, see Gerringa et al., 2015a). Samples were taken east and west of the Ross Sea, in the ACC, and in the Ross Sea. We entered the Ross Sea from the northeast on 20 December and left on the northwestern side on 5 January (Figure 1). Sixty-six samples for ligand analyses were taken at 14 stations in the ACC east of the Ross Sea (East ACC) during the transit along 65° S at 83° W to 149° W (St. 2-9) and between 65° S and 75° S at 149° W to 157° W (St. 10-15). Samples were generally taken in the upper 300 m, with the exception of St. 15, where greater depths were also sampled. Eleven samples were sampled at three stations in the eastern ice-covered Ross Sea (St. 16-18, down to 630 m at St. 16, and the upper 75 m at St. 17 and 18). In the RSP and adjacent ice edge areas, 97 samples at 22 stations were taken from the surface to the bottom, varying between 273 m (St. 61 at the Pennell Bank) and 753 m (St. 45 at the Ross Trough). Thirteen samples were taken at seven stations in the ACC between 63° S and 65.5° S and 159.5° E and 174° E (West ACC), of which 12 were in the upper 50 m; one deep sample was taken at St. 150 (1600 m depth). The central Ross Sea transect (Figure 1 inset) started 10 km from the Ross Ice Shelf along the 177.5˚E meridian to the north, crossing one trough to the Ross Bank and crossing a second trough to the Pennell Bank (St. 20-60), turning west from the Pennell Bank to the Joides Trough (St.61-65), and bending south-west to the south-east (via St. 87, 91 and 101). A separate small section was sampled from 9.5 km east of Franklin Island eastwards (St. 88-90). These were the only stations in the central Ross Sea with sea ice cover (30-50%). Stations 88-90, comprising ten samples, are not part of the transect

(shown in Figures 2-3 and 5), but are incorporated in the calculations of averages shown in Table 2.

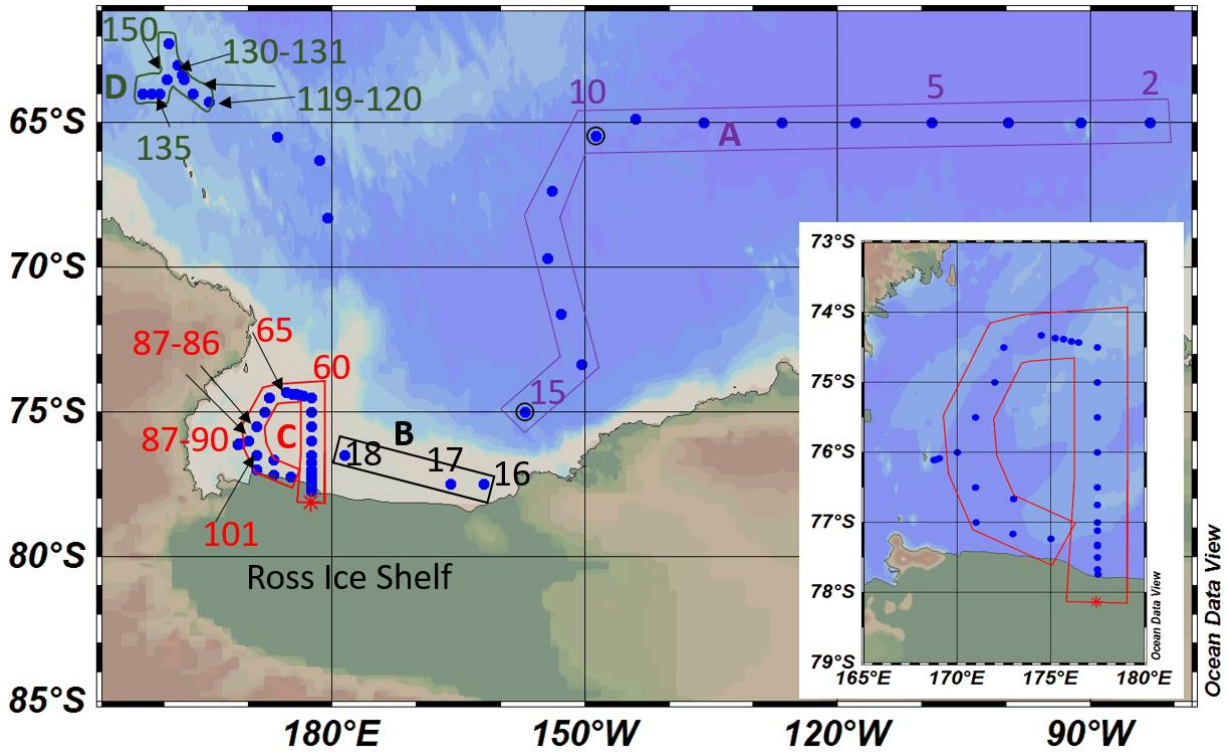

Figure 1 *The ACC and Ross Sea study area. The four transects are: A: the east ACC (EACC) in purple (st. 2-15); B: the east ice covered Ross Sea (ERS) in black (st. 16-18); C: the circle transect in the Ross Sea Polynya (RSP) in red (st. 20-101); see also Inset, and D: the west ACC (WACC) in green (st. 119-150).*

Modified 12 L Go-FLO (Oceanics) samplers provided by the Royal NIOZ (the Netherlands) were attached to a trace metal clean (TMC) frame provided by the United States Antarctic Program on a Kevlar cable. Temperature, depth, and salinity were measured with a SBE 9/11*plus* conductivity-temperature-depth (CTD) system (SeaBird Electronics). The frame also included a C-star transmissometer (WET Labs) and a chlorophyll *a* (Chl *a*) fluorometer (WET Labs). CTD information including conservative temperature (Θ in ˚C) and absolute salinity (S_A in g kg^{-1}) (transformed according to McDougall et al., 2009) are given in Gerringa et al. (2015a).

Typical sample depths were 10, 25, 50, 75, 100, and every 100 m thereafter, depending on water depth.

Water was sampled and filtered (Sartorius®, 0.2 μm; Sartobran 300) for the determination of the DFe and DFe-binding organic ligand characteristics (see below) inside a trace metal clean van. Bottles were rigorously cleaned in three steps according to Geotraces protocols: they were sequentially soaked in detergent (Micro 90®), 6 M HCl (Analar, NormaPur), and filled with diluted acid in between rinsing with milliQ water. Bottles were filled and stored in a 0.35 M HNO_3 solution (Teflon distilled) for DFe analysis and with a 2‰ HCl solution (Merck, Suprapur) for the analysis of the ligand parameters, the latter in order to reduce Fe adsorption onto the bottle wall after sampling.

2.2. Analyses

2.2.1. DFe determination

Trace metal clean work was done in a plastic bubble on the ship. Overpressure in the bubble was achieved by inflow of air through a HEPA filter. Sample handling was done within a laminar flow bench inside the bubble.

DFe concentrations were measured directly on board by the automated Flow Injection Analysis (FIA) method (Klunder et al., 2011) after being acidified for at least 18 hours (Seastar© baseline hydrochloric acid; pH 1.7). Table 1A shows comparison of our analysis of SAFe standards with consensus values. Two subsamples for DFe were taken, one sample was filtered and acidified directly from the Go-FLO bottles (hereafter the concentrations measured in this way are given as DFe), the other was collected from the DFe-binding organic ligand sample bottles (low-density polyethylene) at the time of voltammetric analysis and then acidified as described above (hereafter, the concentrations measured in this way are given as DFe_{Lig}). The samples for the DFe-binding organic ligand characteristics were not acidified, since the partitioning of Fe among its different species, the inorganic and organic complexes, depends on pH. However, in non-acidified samples, Fe adsorbs onto the bottle wall. In order to obtain the DFe present during analysis of the ligand characteristics, DFe_{Lig} was sampled just before this analysis and used for the calculation of the ligand characteristics. Gerringa et al. (2015b) found 13% of DFe from the Western Atlantic was lost on the bottle wall between original sampling and analysis of the ligands. Here the mean DFe_{Lig}/DFe ratio (N=178) is 1.17 (Table 2); however, this ratio is influenced by the sampling strategy. In the present research, most samples were taken

from the upper 100 m where concentrations were very low (N=100 <0.1 nM) rather than being distributed over the depth of an open ocean water column, as in Gerringa et al. (2015b).

2.2.2. Organic complexation of Fe

Organic complexation of Fe was determined in filtered samples by CLE-CSV using 2-(2-Thiazolylazo)-p-cresol (TAC) as a competing ligand (Croot and Johansson, 2000). CLE-CSV was performed using two setups consisting of a μAutolab potentiostat (Metrohm Autolab B.V., formerly Ecochemie, The Netherlands), a 663 VA stand with a Hg drop electrode (Metrohm) and a 778 sample processor with ancillary pumps and dosimats (Metrohm), all controlled using a consumer laptop running Nova 1.9 (Metrohm Autolab B.V.). The VA stands were mounted on elastic-suspended wooden platforms in aluminum frames developed at the NIOZ to minimize ship motion-induced vibration while electrical noise and backup power was provided by Fortress 750 UPS systems for spike suppression and line noise filtering (Best Power). Sample manipulations were performed in laminar flow cabinets.

The competing ligand TAC with a final concentration of 10 μM was used and the complex $(TAC)_2$-Fe was measured after equilibration (> 6 h) at natural seawater temperatures (2°C) in the dark. The increments of Fe concentrations used in the titration were 0, 0.2, 0.4, 0.6, 0.8, 1.0, 1.2, 1.5, 2, 2.5, 3, 4, 6, and 8 nM. The binding characteristics of DFe-binding organic ligands, the ligand concentration [Lt] (in nano-equivalents of M Fe, neq M Fe) and the conditional binding strength K′ (M^{-1}), commonly expressed as logK′, were calculated from the electrical signal recorded (nA) and the DFe_{Lig} concentration using the non-linear regression of the Langmuir isotherm (Gerringa et al., 1995, 2014). LogK′ is expressed with respect to inorganic Fe (Fe′) and 10^{10} is used as the inorganic side reaction at the pH=8.04 of the buffer (Hudson et al., 1992; Liu and Millero, 2002).

The DFe-binding organic ligand characteristics were calculated with two models, one assuming the presence of one ligand group and the other assuming the presence of two ligand groups (Gerringa et al., 2014).

The side reaction coefficient α_{FeLi} of the organic ligands was calculated with DFe as the product of K′ and the concentration of ligands not bound to Fe, [L′], or the sum of the products of K_i' and $[L_i']$ for two ligand groups if present,

$$\propto_{FeL_i} = \sum_i^n K'_i * [L'_i] = \sum_i^n [FeL_i]/[Fe'], \qquad \text{Equation 1}$$

where α_{FeLi} reflects the complexation capacity of the dissolved organic ligands to bind with Fe, which can be seen as its ability to compete for Fe with other ligand groups (also the competing ligand TAC) and with adsorption sites on particles. The parameter α_{FeLi} is a more robust metric for characterizing the DFe-binding organic ligands than K′ and [L′] separately because the Langmuir equation does not treat K′ and [L′] independently from each other (Gledhill and Gerringa, 2017). If an analytical error forces an underestimation of one, the other is automatically overestimated (Hudson et al., 2003). The ratio $[L_t]$/DFe indicates the saturation of the ligands, which are saturated with Fe when the ratio is ≤1 and unsaturated when the ratio is >1 (Thuróczy et al., 2010).

Table 1: Analytical precision of Fe and nutrient analyses: A: comparison of SAFe standards, (bottle number indicated), for the DFe analyses with Flow Injection Analysis (FIA), concentrations in nM (Johnson et al., 2007). B: Precision, accuracy and detection limit of the nutrient determinations.

Table 1A

Standard	#no	consensus	SD	DFe with FIA	SD	number
		nM		nM		
SAFeS	173	0.093	0.008	0.071	0.01	18
SAFED2	94	0.933	0.023	1.012	0.015	9

Table 1B

	PO_4	**Si**	**NO_3**	**NO_2**
	µM	**µM**	**µM**	**µM**
Precision (n=35)	0.01	0.09	0.07	0.006
Accuracy (n=35)	0.001	0.37	0.32	0.02
Detection Limit	0.006	0.06	0.08	0.006

2.2.3. Other chemical analyses

Samples were filtered as described above; separate samples were taken for silicate ($Si(OH)_4$) which were stored at 4°C and for nitrate (NO_3^-), nitrite (NO_2^-) and phosphate (PO_4^{3-}) which were stored frozen. After the cruise, nutrient samples were analysed colorimetrically on a Bran and Luebbe trAAcs 800 Autoanalyzer in the NIOZ nutrient laboratory (Murphy and Riley, 1962; Strickland and Parsons, 1968; Grasshoff et al., 1983). Measurements were made on four channels: PO_4^{3-}, $Si(OH)_4$, NO_3^- and NO_2^- together, and NO_2^- separately. All measurements were

calibrated with standards diluted in low nutrient seawater, which was also used as wash-water between the samples. Detection limits, accuracy and precision are listed in Table 1B, whereas the data can be found in doi:10.25850/nioz/7b.b.g.

Seawater samples for chlorophyll *a* and phaeopigments were filtered onto 25 mm Whatman GF/F filters (nominal pore size 0.7 µm), extracted overnight at 4°C in 5 ml of 90% acetone, and analyzed on a Turner Model 10AU fluorometer before and after acidification (Holm-Hansen et al., 1965).

2.2.4. Statistical considerations

The samples were divided into groups for statistical purposes:

A. Six groups related to sampling depth : <54 m, 54-105 m, 105-205 m (most samples are close to 200 m), 205-305 m (most samples are close to 300 m), 305-405 m (most samples are close to 400 m), >450 m (most samples are close to 500 m).
B. Three groups related to mixed layer depth (MLD, defined as a change in neutral density of 0.02 $kg.m^{-3}$): in; under (=MLD+30 m); out. The group "under" was made as a test to get the layer where grazing might be important.

Pearson product-moment correlation scores (r) were calculated between ligand parameters and other parameters (e.g., Chl *a* and phaeophytin, nutrients, phytoplankton species, presence in the MLD, water mass type and transect) using the software package R. A MANOVA test was executed using SPSS between the presence of one or two DFe-binding organic ligand groups and phytoplankton species composition (Alderkamp et al., in press). The division B did not give significant results and will thus not be discussed.

3. Results

3.1 Hydrography

Gerringa et al. (2015a) described the four water masses present in the circle transect in detail so only a brief summary is provided here. AASW, Winter Water (WW), Shelf Water (SW), and mCDW were distinguished using the definitions of Tomczak and Godfrey (2001) and Orsi and Wiederwohl, (2009); the determining temperature properties are indicated as contours in Figure 2. AASW is surface water, defined by potential temperatures (Θ) >−1.85 °C and neutral density <28 kg m^{-3}, WW is cold remnant water of the previous winter, whereas AASW has been warmed at the surface. Only north of 76°S (St. 48) WW was found . Near the Ross Ice

Shelf cold SW is formed, Θ<−1.85 °C, with variable salinity depending on salt rejection, with sub-divisions in Ice SW (ISW) Θ<−1.95 °C and high and low salinity SW (S> or < 34.62). At the southern stations (St. 16, 17, 20 and 44) ISW was recognized (Figure 2B and C). From the north mCDW enters the Ross Sea shelf which is characterized by elevated temperatures, and salinities between 34 and 35 and was present predominantly in the north under the AASW until the bottom (St. 60). Due to mixing and modification mCDW was difficult to recognize beyond 76° S in the western section (south of St. 65) of the circle transect and beyond 75° S in the eastern part of the circle transect (near St. 48) (Figure 2C).

The upper 100-150 m in the East and West ACC transects consisted of AASW and CDW was found below. North of 64° S in the western transect, cold sub-zero WW was found near the surface together with AASW , with surface temperatures >0°C (between St. 119 and 135) (Figure 2A, D).

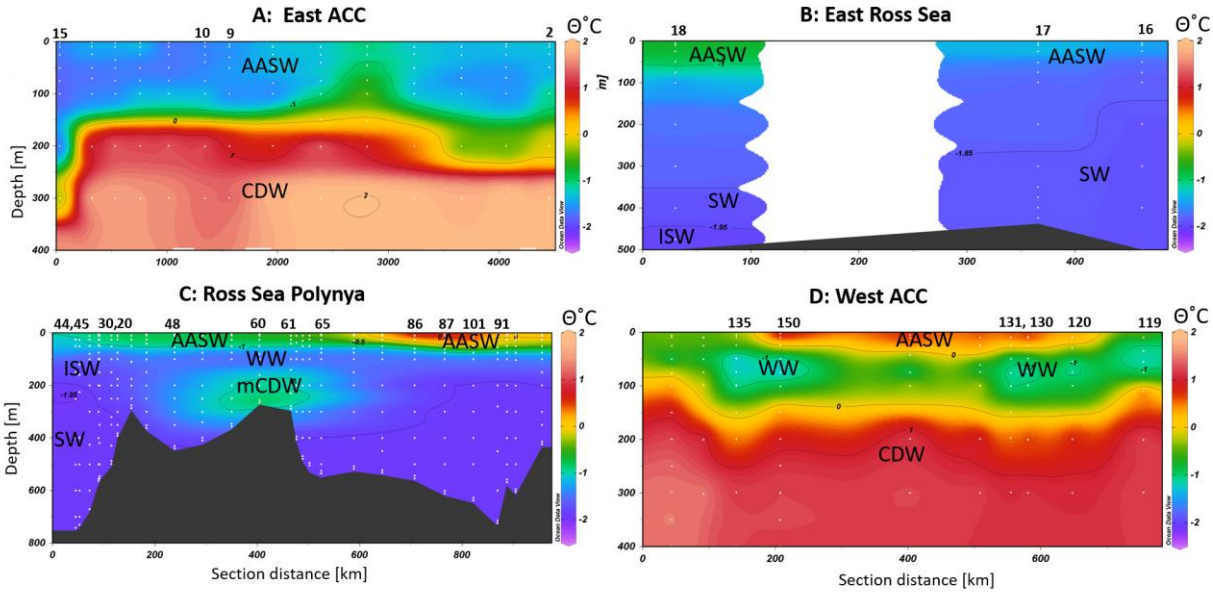

Figure 2: *Conservative temperature (degrees C) along the four transects. A: east ACC, B: east ice covered Ross Sea, C: circle transect RSP, D: west ACC. The contours indicate water mass defining temperatures. AASW: Antarctic Surface Water; CDW: Circumpolar Deep Water; ISW: Ice Shelf Water; mCDW: Modified Circumpolar Deep Water; SW: Shelf Water and WW: Winter Water. Ligand samples have been collected at stations indicated.*

The MLD varied between 8 and 99 m, and had a mean depth of 36 m (±21 m). High values (>70 m) occurred in the Ross Trough (stations 30, 43, 44, 45,and 46). Low values

occurred near Franklin Island (stations 87-90), where the MLD was between 8 and 10 m. Above the bottom in the circle transect a BNL could be distinguished in some of the stations by a decrease in transmission (Gerringa et al., 2015).

3.2. Nutrients and fluorescence

Nutrient concentrations (doi:10.25850/nioz/7b.b.g) were relatively low in the surface (8-20 µM NO_3^-; 0.3-1.4 µM PO_4^{3-}; 25-45 µM $Si(OH)_4$) and increasing with depth to 32 µM NO_3^-, 2.2 µM PO_4^{3-} and 90 µM $Si(OH)_4$ in the Ross Sea and 110 µM $Si(OH)_4$ in the West ACC. Nutrient concentrations were low where fluorescence (Figure 3) and Chl *a* (not shown) were elevated in the southern part of the circle transect in the RSP and in the West ACC at stations 120, 130, 131 and 150 (doi:10.25850/nioz/7b.b.g). The lowest concentrations were measured at the surface at St. 87 and 86, with 8 and 13 µM NO_3^-, 0.34 and 0.6 µM PO_4^{3-}, and 33.6 and 42 µM $Si(OH)_4$ (not shown), respectively, but not so low as to be limiting phytoplankton growth (Alderkamp et al., 2019). However, lower $Si(OH)_4$, but still non-limiting, was observed in the surface water of the East ACC transect between 25 and 33 µM at St 2-6.

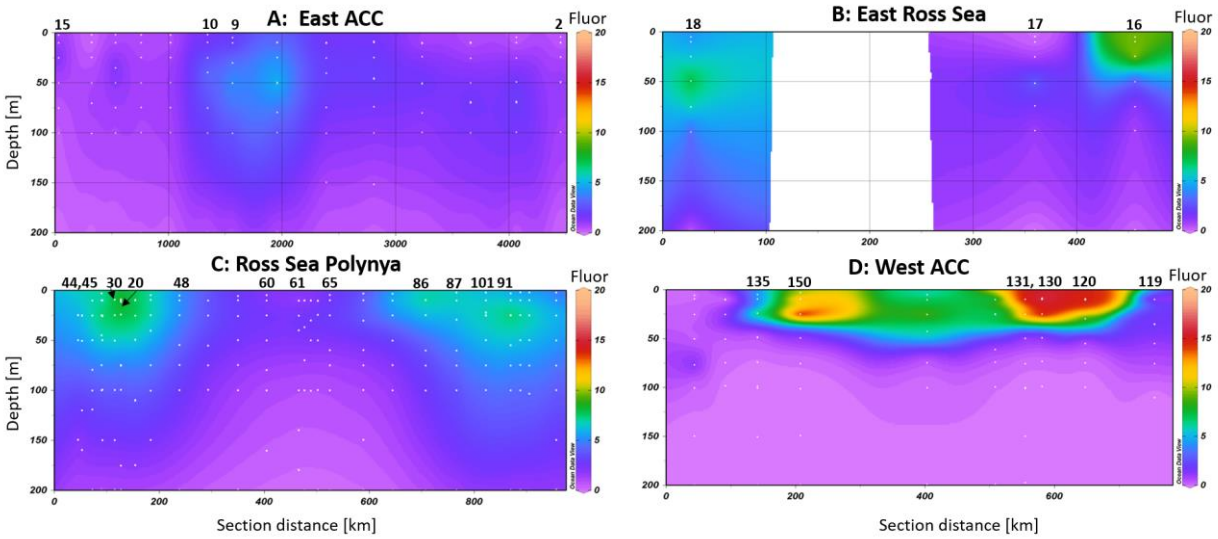

Figure 3*: Fluorescence profiles (a.u.) along the four transects in the upper 200m. A: East ACC, B: East ice covered Ross Sea, C: circle transect in the RSP, D: West ACC.*

***Table 2**: Median and average values of DFe and the DFe-binding organic ligand parameters for all samples and per transect when the one ligand model is applied (logK´, $[L_t]$ and excess DFe-binding organic ligand concentration [L´]) and when a two ligand model is applied ($logK´_1$, $logK´_2$, $[L_1]$ and $[L_2]$). The standard deviation (SD) of the average, the maximum (Max) and minimum (Min) values are given and the number of samples (N). DFe (nM) was measured in immediately acidified samples and DFe_{Lig} (nM) was measured in samples from the ligand sample bottle. ΣL_1L_2 means the sum of $[L_1]$ and $[L_2]$. DFe-binding organic ligand concentrations are expressed in neq M Fe, K' in M^{-1}, α_{FeLi} is dimensionless, the ratios of $[L_t]$ and DFe are dimensionless.*

	DFe nM	DFe_{Lig} nM	DFe_{Lig}/DFe	logK'	$[L_t]$ neq M Fe	[L'] neq M Fe	$\log\alpha_{FeLi}$	$logK'_1$	$logK'_2$	$[L_1]$ neq M Fe	$[L_2]$ neq M Fe	ΣL_1L_2 neq M Fe	$\Sigma L_1L_2/[L_t]$	$[L_t]$/DFe	ΣL_1L_2/DFe
All															
Median	0.097	0.090	0.95	12.24	1.08	0.90	3.16	13.48	11.19	0.60	1.02	1.53	1.16	9.67	13.83
Mean	0.192	0.192	1.17	12.29	1.11	0.93	3.11	13.57	11.14	0.58	1.06	1.64	1.21	6.52	24.27
SD	0.339	0.226	0.74	0.34	0.42	0.45	0.60	0.48	0.19	0.20	0.43	0.52	0.26	17.49	22.31
Max	2.338	1.740	4.74	13.38	2.61	2.49	4.20	15.26	11.54	1.01	2.58	3.40	2.68	101.43	104.00
Min	0.012	0.011	0.20	11.58	0.31	0.001	0.99	12.61	10.39	0.10	0.27	0.68	0.52	0.45	1.51
N	176	185	176	185	185	185	185	72	72	72	72	72	72	186	72
East ACC															
Median	0.071	0.0685	0.95	12.24	0.85	0.71	3.06	13.44	11.02	0.41	0.92	1.20	1.18	8.87	10.61
Mean	0.100	0.090	1.10	12.27	0.83	0.73	3.10	13.26	11.01	0.42	1.05	1.47	1.29	17.62	33.29
SD	0.079	0.068	0.67	0.39	0.29	0.29	0.35	0.46	0.32	0.20	0.64	0.78	0.59	20.57	39.97
Max	0.324	0.327	3.79	13.38	1.42	1.41	4.22	13.70	11.54	0.82	2.58	3.40	2.68	101.43	104.00
Min	0.012	0.011	0.20	11.58	0.31	0.25	2.29	12.61	10.39	0.10	0.27	0.68	0.52	1.76	4.04
N	63	64	63	64	64	64	64	9	9	9	9	9	9	64	9
East ice covered Ross Sea															
Median	0.130	0.083	0.84	12.20	0.83	0.65	2.95	13.32	10.93	0.34	0.84	1.18	1.11	7.41	19.03
Mean	0.235	0.197	0.85	12.24	0.82	0.61	2.80	13.32	10.93	0.34	0.84	1.18	1.11	7.58	19.03
SD	0.250	0.241	0.18	0.21	0.16	0.28	0.73	NA	NA	NA	NA	NA	NA	5.09	NA
Max	0.707	0.682	1.12	12.62	1.06	1.21	3.45	13.32	10.93	0.34	0.84	1.18	1.11	17.10	19.03
Min	0.067	0.051	0.52	11.99	0.58	0.001	0.70	13.32	10.93	0.34	0.84	1.18	1.11	0.84	19.03

N	10	11	10	11	11	11	11	1	1	1	1	1	1	11	1
RSP															
Median	0.122	0.114	0.94	12.22	1.24	1.05	3.24	13.53	11.18	0.60	1.02	1.51	1.16	9.67	13.41
Mean	0.267	0.213	1.17	12.30	1.26	1.03	3.11	13.64	11.14	0.58	1.06	1.63	1.20	14.52	21.29
SD	0.446	0.284	0.79	0.34	0.40	0.47	0.71	0.51	0.16	0.20	0.40	0.47	0.18	14.44	18.78
Max	2.338	1.740	4.74	13.19	2.61	2.49	4.16	15.26	11.41	1.01	2.09	3.05	1.74	71.42	73.24
Min	0.024	0.034	0.35	11.63	0.39	0.001	0.99	12.83	10.72	0.21	0.34	0.92	0.76	0.45	1.51
N	91	97	91	97	97	97	97	52	52	52	52	52	52	98	52
West ACC															
Median	0.043	0.087	1.72	12.33	1.54	1.50	3.48	13.45	11.27	0.74	1.07	1.81	1.15	35.0	30.01
Mean	0.076	0.129	1.85	12.33	1.56	1.48	3.49	13.49	11.27	0.75	1.12	1.87	1.22	33.74	32.20
SD	0.111	0.120	0.65	0.16	0.19	0.24	0.13	0.22	0.04	0.07	0.45	0.46	0.21	18.85	17.36
Max	0.426	0.414	3.50	12.63	1.91	1.88	3.71	13.82	11.36	0.90	2.20	3.00	1.75	73.46	54.59
Min	0.026	0.060	0.89	12.10	1.17	0.96	3.31	13.15	11.21	0.65	0.50	1.24	1.06	3.26	4.41
N	12	13	12	13	13	13	13	10	10	10	10	10	10	13	10

3.3 Fe and ligand parameters

Mean and median values were calculated for all samples, per transect, per depth layer and per depth layer per transect (Table 2, Figure 4). For [L_t] and DFe the median and mean values were similar with one exception for DFe in the East Ross Sea. At St. 17 an unusual high DFe was measured at 300 m (1.242 nM). This concentration was considered an outlier (illustrated in Figure 4B) and not used in Table 2. The DFe varied between extreme low concentrations in the surface (upper 54 m) and relatively high concentrations near the sediment in the RSP (0.012 to 2.338 nM). The DFe-binding organic ligand concentration [L_t] varied between 0.31 and 2.61 with a mean of 1.1 neq M Fe (SD 0.42, N=185). Low values for [Lt] occurred predominantly in the eastern sections (Figure 4A). In the RSP and in the West ACC, [L_t] was higher (mean [L_t] = 1.26 and 1.56 respectively, Table 2, Figures 4A and 5A). Although logK′ varied between 11.58 and 13.38; the mean logK′ did not vary between transects and depths and was consistently between 12.24 and 12.3. The value of logα_{FeLi} varied between 0.60 and 4.2, with mean values of 3.10 in the East ACC, 2.80 in the East Ross Sea, 3.11 in the RSP, and 3.49 in the West ACC. The mean values with depth (Figure 5B) per transect show very low DFe in the surface (<0.1 nM), increasing with depth in all sections. The large increase in the Ross Sea below 300 m was due to the presence of a BNL (Gerringa et al., 2015a).

Little variation with depth in mean [Lt] was observed. The mean [Lt] was lower in the ice covered East Ross Sea and the East ACC than in the RSP and West ACC, with a minimum at 200 m in the East ACC. One deep sample was taken in the West ACC, at St. 150 at 1600 m, where [L_t] = 1.39 neq M Fe (see also figure caption Figure 4). The ratio [Lt]/DFe and logα_{FeLi} decreased with depth because of increasing DFe and constant [Lt] (Figures 4 and 5). Due to the increasing DFe, the DFe-binding organic ligands became more saturated with depth, resulting in a decrease in [L′] and since logK′ remained constant, also a decrease in logα_{FeLi}. In the RSP BNL where DFe >1 nM, the ligands were saturated with Fe, causing the ratio [Lt]/DFe to be <1 in some samples. The deep sample at St. 150, which was still far above the sediment, had relatively low DFe concentrations (0.426 nM) and the ligands were not saturated as shown by [Lt]/DFe =3.26. The value of logα_{FeLi} (3.37) was close to the mean value in the upper 50 m of the West ACC

Of the 185 samples we collected, 72 contained two ligand groups (Table 2 and Figure 5D). This means that for these samples, a one ligand model as well as a two ligand model could

be fit. By convention, a number 1 is assigned to the strongest ligand group and a number 2 to the weaker ligand group. The mean values were $\log K'_1$ =13.57 (SD=0.48), $\log K'_2$=11.14 (SD=0.19), $[L_1]$ = 0.58 (SD=0.24), $[L_2]$ =1.06 (SD=0.43) neq M Fe (Table 2). From previous work, we know that the two ligand model for data obtained with TAC as a competing ligand can result in a disagreement between the two models ($[L_1] + [L_2] \neq [Lt]$), casting doubt on the two ligand model data (Slagter et al., 2019). In the present study, 51 out of 72 samples (70%) gave a good correspondence between the two models, as indicated by the ratio $[L_1] + [L_2]/[L_t]$ being close to 1 (Table 2). Per region, the percentage of samples where the two ligand model fitted the data differed. Two ligand groups could be distinguished in 15% of the samples from the East ACC, 10% from the East Ross Sea, 54% from the RSP, and 77% from the West ACC (Table 2). The West ACC was only sampled in the surface 54 m, except for one sample at 1600 m, which also showed two ligand groups. In the RSP, two ligand groups were found over the whole water column, except in the high DFe BNL (Figure 5D).

4. Discussion

4.1 The one ligand model

The values of $\log K'$ and [Lt] we measured overlap with work of others done in Antarctic waters (Boye et al., 2001; Thuróczy et al., 2011, 2012). Rivaro et al. (2018) detected DFe-binding organic ligands with higher $\log K'$ (12.1-12.6) in a coastal area near Terra Nova Bay in the Ross Sea where DFe was elevated (0.52-5.41 nM). Since they used another competing ligand (2,3-dihydroxynaphtalene) with a higher analytical window than we did, this might explain their higher $\log K'$. Although the coastal influence of Terra Nova Bay could provide another more probable explanation. We did not see higher logK' in the present study at coastal stations near Franklin Island (St. 88-90).

4.1.1 Relationships between ligands and phytoplankton

Although the ligand concentration $[L_t]$ was higher in areas with high phytoplankton abundance, we found no significant correlation between $[L_t]$ and Chl *a*, fluorescence, phytoplankton species and MLD in our data set (best correlations were for fluorescence versus $[L_t]$ (p=0.055) and for Chl *a* versus $[L_t]$ (p=0.195). DFe-binding organic ligands are released during grazing and this source of ligands is recently shown to be important for the recycling of

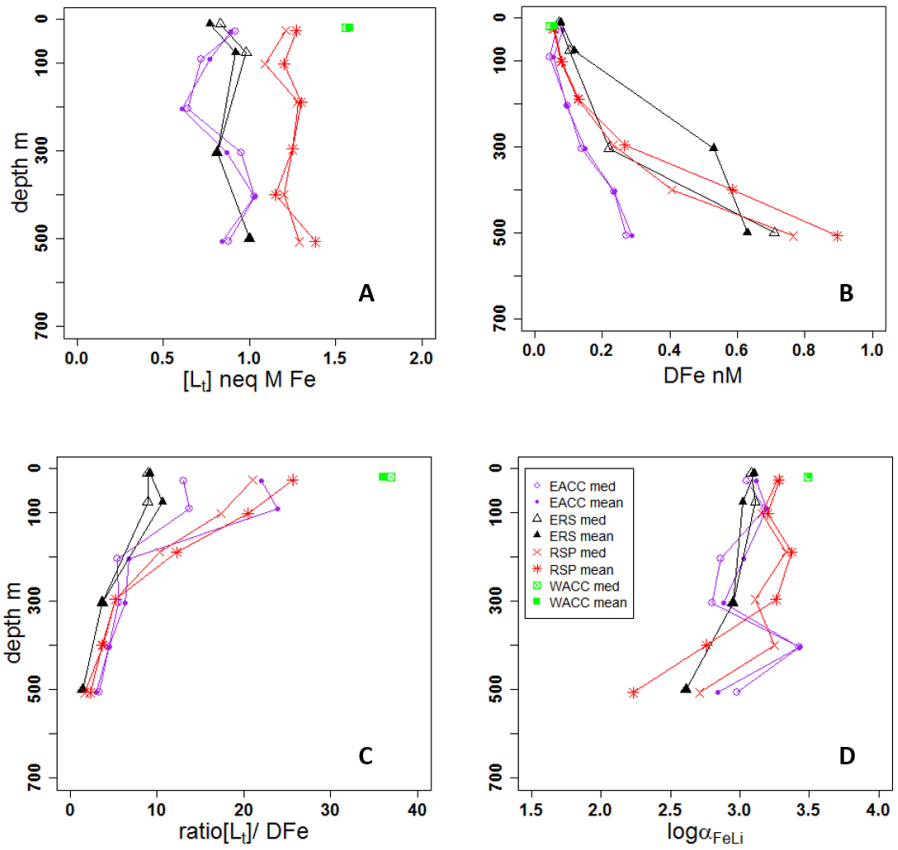

Figure 4: *Median and mean values over depth sections per transect for A: [Lt] (neq M Fe), B: DFe (nM), C: the ratio [Lt]/DFe, D: logα_{FeLi}. The depth sections are upper 54 m, 55-105 m, near 200 m, near 300 m, near 400 m and >450 m. One deep observation in the west ACC at 1600 m is not shown and has [Lt] = 1.39 neq M Fe, DFe= 0.426 nM, [Lt]/DFe =3.26 and logα_{FeLi} = 3.37.*

DFe in Antarctic waters (Laglera et al., 2019). We did not measure zooplankton or grazing during the cruise. However, phaeophytin, a phaeopigment which is a breakdown product of Chl *a*, is sometimes used as a tracer for grazing (SooHoo and Kiefer, 1982). Although grazing pressure cannot be simply estimated by phaeopigment measurements (Gieskes et al., 1991) we used phaeophytin as a raw indicator of grazing. Pearson correlation shows that in the East ACC and the RSP, weak correlations existed between [L_t] and both Chl *a* and phaeophytin (R = 0.34 - 0.50). Interestingly, the correlation with both pigments (Chl *a* and phaeophytin) was positive in the East ACC in the upper 54 and 105 m, but negative between [Lt] and phaeophytin in the upper 54 m of the RSP. The phaeophytin concentration was not particularly high (results not shown). Grazing is reported to be relatively low in the Ross Sea and thus might play a less important role here as elsewhere in the Southern Ocean and Antarctic seas (Smith et al., 2000; Tagliabue and

Arrigo, 2003). Both Chl *a* and phaeophytin were never measured below 100 m where they are expected to be very low since fluorescence is very low below the upper mixed layer (Figure 3). Positive as well as negative correlations between [L_t] and phytoplankton pigments illustrate how difficult it is to find a relationship between ligands and primary production in the oceans (Rue and Bruland, 1995; Gerringa et al., 2006; Buck et al., 2015; Hassler et al., 2017), despite the fact that production of ligands by biota is evident from experiments (Butler, 2005; Poorvin et al., 2011; Velasquez et al., 2016).

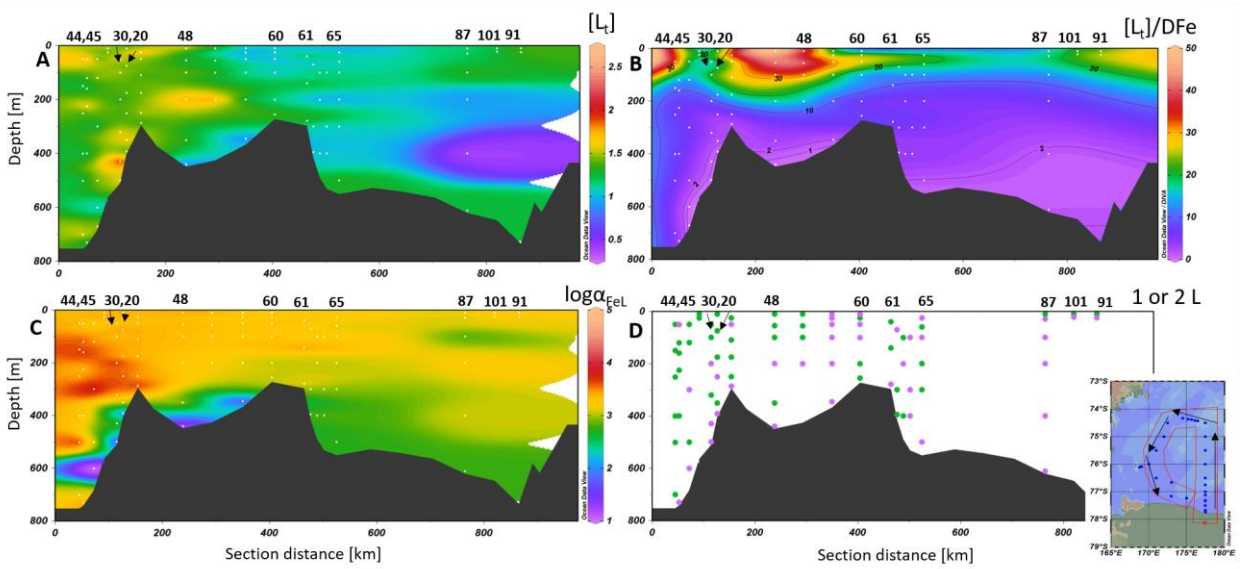

Figure 5: *Parameters of the circle transect in the RSP. A: [Lt] in neq M Fe, B: the ratio [Lt]/DFe with contours at the values [Lt]/DFe 1, 2, 10, 20 and 30, C: logα_{FeL} and D: Green dots indicate samples where 2 DFe-binding ligand groups could be distinguished and purple dots where 1 DFe-binding ligand group was found. In the right hand corner a map showing the circle transect (see also Figure 1). Arrows indicate the order from left to right in the transect plots A-D.*

Many processes influence the DFe-binding organic ligand concentrations in major phytoplankton blooms such as we encountered in the RSP and West ACC. During these blooms, phytoplankton grow rapidly until the bloom reaches a stationary phase, after which the phytoplankton biomass declines (Alderkamp et al., 2007; Arrigo et al., 2015). Several processes may be responsible for the decline, most of which can affect ligand concentrations. Ligands are produced by phytoplankton and bacteria through excretion of organic substances, especially upon Fe limitation (Butler, 2005; Boiteau et al., 2016), which we encountered at the time of

sampling (Alderkamp et al., 2019). In addition, ligands are released by grazing (Sarthou et al., 2008; Laglera et al., 2017, 2019) and viral lysis (Poorvin et al., 2011). On the other hand, ligand concentrations decline by photo-oxidation (Barbeau, 2006), bacterial degradation (Hassler et al., 2011; Velasquez et al., 2016) and coagulation and sinking. Apparently, in the RSP the combination of these processes of production and loss together with turbulent mixing (the MLD can extend to 500 m in early spring (Smith et al., 2000)), resulted in depth profiles of more or less constant DFe-binding organic ligand concentrations (Figure 4A).

According to Ducklow (2003) labile and semi-labile (short-lived) dissolved organic matter (DOM) produced in the RSP is broken down by bacteria within the growing season and thus labile DOM is expected to be mainly restricted to the upper water layer, the MLD and just below (Laglera et al.; 2019; Gerringa et al., 2006). We did not observe elevated DFe-binding organic ligands in the surface 50-100 m, and neither in the 'under the MLD' layer (section 2.2.4), similar to other studies in the Southern Ocean (Thuróczy et al., 2011) and elsewhere (Buck et al., 2015; Gerringa et al., 2015b;), although elevated DFe-binding organic ligands in the upper 100 m have been observed in the Southern Ocean (Boye et al., 2001;Thuróczy et al., 2012) and elsewhere (Gerringa et al., 2006). It may be that we missed part of the labile DFe-binding organic ligands that are easily degradable such as the very photo-labile siderophores (Amin et al., 2012). Therefore we probably mostly measured the DFe-binding organic ligands fraction that is relatively resistant to degradation, which are mixed through the water column in autumn and are also transported with high salinity SW into the Southern Ocean (Jacobs and Giulivi, 1999; Smith et al., 2000; Gordon et al., 2009).

4.1.2 Relations between ligands and water mass, sediments and sea ice

No correlations were found between water mass and ligand concentration [L_t]. The deep maxima in DFe together with reduced transmission in the RSP indicate the presence of a BNL (Gerringa et al., 2015a). However, these maxima do not coincide with high DFe-binding organic ligand concentrations, implying that the BNL is only a source of Fe and not of ligands. Our analysis method used TAC as competing ligand, which can miss part of the humic DFe-binding ligands (Laglera et al., 2011, Slagter et al., 2019; Dulaquais et al., 2018). Therefore it is possible that the ligands are underestimated if humic-like substances are present, which might be the case in the BNL. In humic rich surface waters of the Arctic [L_t] estimated with TAC did increase with

the humic content, but [L_t] was lower than DFe and lower than [L_t] obtained with salicylaldoxime (SA, Rue and Bruland, 1995; Buck et al., 2015). According to Slagter et al. (2019) the method using TAC detects humic-like substances only at high concentrations or only of specific composition. Thus in this research we cannot exclude the BNL as a possible source of DFe-binding organic ligands, we can only conclude that the BNL is probably not a large source.

Another important DFe-binding organic ligand source in Antarctic waters is ice melt. Lannuzel et al. (2015) showed that the solubility of Fe in sea ice, snow, and brines was controlled by the presence of organic ligands, with high concentrations of up to 80 neq M Fe, and with the same logK' as in seawater. Recently, Genovese et al. (2018) made similar observations in east Antarctic pack ice. Ice algae and bacteria are considered to be the ligand source and when the ice melts, Fe and ligands are released into the ocean where the ligands continue to play a role in maintaining Fe solubility (Lannuzel et al., 2015). The eastern Ross Sea stations (St. 16-18) had sea ice cover, which had probably started melting, but this did not result in increases in [Lt] in the upper 54 m. The stations sampled near Franklin Island had 30-50% ice cover, but [Lt] was comparable to values in ice free zones (1.2-1.3 neq M Fe) (St. 88, 89, 90). Even at the borders of the polynya, where sea ice was melting this did not result in detectable elevations of DFe-binding organic ligands. It is difficult to assess the role of melting sea-ice in the present study. Brine drainage, occurring in specific short periods releasing DFe into the underlying water (Lannuzel et al., 2008), also possibly plays a role in the release of DFe-binding organic ligands.

We did not find evidence of photo-oxidation of DFe-binding organic ligands (Barbeau, 2006) since ligand concentrations in ice covered stations were lower compared to stations in the polynya and open ocean (stations 16-18 and 88-90 had average [Lt] of 0.85 and 1.01 neq M Fe respectively, versus 1.25 neq M Fe in the RSP).

4.2 The two ligand model

The ability to detect two ligand groups may be related to the specific analytical method used. Multiple ligand groups are found much more often using SA as competing ligand in the CLE-CSV technique than when using TAC (Bundy et al. 2015; Buck et al. 2016; Slagter et al., 2019). One of the reasons might be that TAC misses part of the humic-like substances as discussed above. Because of the distance to the continent, together with the lack of soil

formation in the Antarctic climate, we assume that humics do not play a major role in the RSP with the possible exception of the BNL, and therefore it is likely that underestimates, if any, of concentrations of the ligand groups outside the BNL are small.

An important problem in identifying two ligand groups is related to data quality and interpretation. The one ligand model results in ligand characteristics that reflect an average of the binding strengths of groups and molecules that form the mixture of DFe-binding organic ligands Therefore, the logK′ values of the one ligand model are a weighted average of those found for the two ligand model (Table 2). If the ligand concentration not bound to Fe, [L′], is high in the natural sample, more data points are obtained during a titration with Fe using fixed Fe additions than when [L′] is small. More data points give more resolution to detect two ligand groups. At relatively low [L′], the probability of detecting the strongest DFe-binding organic ligand group, L_1, is limited because this ligand group is saturated since it competes most strongly with TAC for ambient Fe. Thus, irrespective of their actual presence, it is unclear whether detecting two ligand groups simply depends on low DFe and a high [L′], and that the strongest ligand is often hidden due to (near) saturation with Fe. Indeed at [L′] < 0.6 neq M Fe, two ligands were not detected in our data. Since in the BNL the ligands were near saturation, two ligands were not detected in this layer. However, this does not mean that high [L′] always resulted in the detection of two ligand groups. In 25 of our samples (N=185), [L′] exceeded 1 neq M Fe and yet only the one ligand model fitted the data. Perhaps only one ligand group existed there, but it might also be that the groups of ligands were not different enough in binding characteristics to be distinguished from each other.

The ligand group L_1 is often described as existing primarily in the surface ocean and is related to sources connected with primary production, such as the siderophores produced in Fe-limited conditions by bacteria (Rue and Bruland, 1995, Bundy et al., 2014; Buck et al., 2015; Gledhill and Buck, 2012). Although these bacteria are present throughout the water column, they exist in higher amounts in the upper 50 or 100 m (Bundy et al., 2016; Velasquez et al., 2016; Hassler et al., 2017). However, in the southeast portion of the circle transect in the RSP very high concentrations of both L_1 and L_2 were found throughout the entire water. Two ligand groups were also found at a depth of 1600 m at St. 150 in the West ACC, indicating a long residence time in the ocean. Although there is likely a relationship between algal blooms and ligand diversity, it is not clear whether there were specific ligand groups produced during the bloom in

this study. A MANOVA test rejected any correlation between the presence of two ligand groups and the occurrence and cell counts of phytoplankton species. Phytoplankton species consisted predominantly of diatoms (61%) and Phaeocystis (33%) (detailed information on phytoplankton species is described by Alderkamp et al. (2019)). Contrasting results are known from literature using the same method for measuring ligands. For example, Bundy et al. (2014), found a correlation of the occurrence of the strongest ligand group with spring blooms while Buck et al. (2015) found that ligand groups were ubiquitous at all depths in the N-E Atlantic Ocean. It is thus not surprising that in our study, the presence of two ligands was unrelated to depth. However, higher [L_t], [L_1], and [L_2] were observed where blooms were present. Processes related to primary production, viral lysis, grazing, and bacterial breakdown of organic matter are all possible sources of Fe-binding dissolved organic ligands, with bacterial breakdown also resulting in a loss of organic ligands. Individual processes can be studied in well-defined bottle experiments, whereas field samples only allow us to study a snapshot of the overall processes, obscuring direct source and sink relationships between biological parameters and ligand concentration and diversity.

5. Conclusions

The concentration of DFe-binding organic ligands in the Ross Sea was responsible for keeping Fe in the dissolved phase and potentially available for phytoplankton growth. Only in the BNL of the RSP was DFe higher than the ligand concentrations and above the solubility product of the Fe-(hydr)oxides. Although our analysis method might have missed part of humic-like substances, the BNL was probably not a source of DFe-binding organic ligands.

The absence of depth related variability of the Fe-binding dissolved organic ligands indicates that the ligand groups we measured were not labile substances and might be transported over the shelf by high salinity SW into the Circumpolar Current. Although the DFe-binding organic ligands measured in this study explain DFe concentrations and enable transport from Fe sources, the labile DFe-binding organic ligands may play an important role in Fe uptake by algae, needing further study.

There was no relationship between DFe-binding organic ligand concentrations and depth or presence in the MLD. No straightforward correlation with other parameters like fluorescence and phytoplankton species was detected. However, the highest concentrations were measured

where primary production was highest. Although the detection of more than one ligand group was not related to phytoplankton species, we conclude that the presence of two Fe-binding organic ligand groups were more common in areas where blooms occurred (54-77% of the samples) than where fluorescence was low (10-15% of the samples)

Acknowledgements

The authors are most grateful to Captain John Souza and crew of R.V.I.B. Nathaniel B. Palmer, all Phantastic participants, as well as the excellent support by the Antarctic Support Contract (ASC) technicians.

The US component of this research was sponsored by the National Science Foundation Office of Polar Programs (Phantastic ANT-1063592 to KRA).

Data is made available upon publication, draft doi:10.25850/nioz/7b.b.g

Martijn van Haren (University Groningen) is thanked for his help with the MANOVA test. Hans Slagter is acknowledged for his help with R.

The comments of two anonymous reviewers considerably improved this paper.

References

Alderkamp, A-C., Buma, A.G.J., van Rijssel, M., 2007. The carbohydrates of Phaeocystis and their degradation in the microbial food web. Biogeochemistry 83, 99-118.

Alderkamp, A-C., van Dijken, G.L., Lowry, K.E., Lewis, K.M., Joy-Warren, H., van de Poll, W., Laan, P., Gerringa, L.J.A., Delmont, T., Jenkins, B., Arrigo .K.R., 2019. Effects of iron and light availability on phytoplankton photosynthetic properties in the Ross Sea. MEPS, 621: 33-50. Https://doi.org/10.3354/meps13000.

Amin S.A., Green D.H., Gärdes A., Romano A., Trimble L., Carrano C.J., 2012. Siderophore-mediated iron uptake in two clades of Marinobacter spp. associated with phytoplankton: the role of light. Biometals, 25,181-92. doi: 10.1007/s10534-011-9495-5.

Arrigo, K.R., van Dijken, G. L., 2003. Phytoplankton dynamics within 37 Antarctic coastal polynya systems. J. Geophys. Res., 108, NO. C8, 3271, doi:10.1029/2002JC001739, 2003

Arrigo, K. R., Worthen, D. L., Robinson, D. H., 2003. A coupled ocean-ecosystem model of the Ross Sea: 2. Iron regulation of phytoplankton taxonomic variability and primary production, J. Geophys. Res., 108(C7), 3231, doi:10.1029/2001JC000856.

Arrigo, K. R., van Dijken, G., Long, M., 2008a. Coastal Southern Ocean: A strong anthropogenic CO2 sink, Geophys. Res. Lett., 35, L21602, doi:10.1029/2008GL035624.

Arrigo, K. R., van Dijken, G. L., Bushinsky, S., 2008b. Primary production in the Southern Ocean, 1997–2006, J. Geophys. Res., 113, C08004, doi:10.1029/2007JC004551.

Arrigo, K. R., G. L. van Dijken, and A. L. Strong, 2015. Environmental controls of marine productivity hot spots around Antarctica, Journal of Geophysical Research, 120, 5545–5565, doi:10.1002/2015JC010888.

Barbeau, K., 2006. Photochemsitry of organic iron(III) complexing ligands in oceanic systems. Phototchem. Phototbiol. 82, 1505-1516. DOI: 10.1562/2006-06-16-IR-935

Boiteau, R.M., Mende, D.R., Hawco, N.J. McIlvin, M.R., Fitzsimmons, J.N., Saito, M.A., Sedwick, P.N. DeLong, E.F., Repeta D.J., 2016. Siderophore-based microbial adaptations to iron scarcity across the eastern Pacific Ocean. PNAS, 113, 14237–14242 www.pnas.org/cgi/doi/10.1073/pnas.1608594113

Boyd, P.W., Jickells, T., Law, C.S., Blain, S., Boyle, E.A., Buesseler, K.O., Coale, K.H., Cullen, J.J., De Baar, H.J.W., Follows, M., Harvey, M., Lancelot, C., Levasseur, M., Owens, N.P.J., Pollard, R., Rivkin, R.B., Sarmiento, J., Schoemann, V., Smetacek, V., Takeda, S., Tsuda, A., Turner, S., Watson, A.J., 2007. Mesoscale iron enrichment experiments 1993-2005: Synthesis and future directions. Science 315, 612-617.

Boye, M., Van den Berg, C.M.G., de Jong, J.T.M., Leach, H., Croot, P.L., de Baar, H.J.W., 2001. Organic complexation of iron in the Southern Ocean. Deep Sea Res. I 48, 1477-1497.

Buck, K.N., Gerringa L.J.A., Rijkenberg M.J.A., 2016. An Intercomparison of Dissolved Iron Speciation at the Bermuda Atlantic Time-series Study (BATS) Site: Results from GEOTRACES Crossover Station A. Front. Mar. Sci. 3:262. doi: 10.3389/fmars.2016.00262

Buck, K.N., Sohst, B., Sedwick, P.N., 2015.The organic complexation of dissolved iron along the U.S. GEOTRACES (GA03) North Atlantic Section. *Deep Sea Res.II* 116,152–165.doi:10.1016/j.dsr2.2014.11.016

Bundy, R.M., Abdulla, H.A.N., Hatcher, P.G., Biller, D.V., Buck, K.N., Barbeau, K.A., 2015.Iron-binding ligands and humic substances in the San Francisco Bay estuary and

estuarine-influenced shelf regions of coastal California. *Mar.Chem.* 173,183–194.doi:10.1016/j.marchem.2014.11.005
Bundy, R.M., Biller, D.V., Buck, K.N., Bruland, K.W., Barbeau, K.A., 2014. Distinct pools of dissolved iron-binding ligands in the surface and benthic boundary layer of the California Current. *Limnol. Oceanogr.* 59,769–787. doi:10.4319/lo.2014.59.3.0769
Bundy, R.M., Jiang, M., Carter, M., Barbeau, K.A., 2016. Iron-binding ligands in the Southern California current system: mechanistic studies. *Front. Mar.Sci.* 3:27.doi:10.3389/fmars.2016.00027
Butler, A., 2005. Marine siderophores and microbial iron mobilization. Biometals 18, 369–374.
Coale, K.H., Gordon, R.M., Wang, X., 2005. The distribution and behavior of dissolved and particulate iron and zinc in the Ross Sea and Antarctic Circumpolar Current along 170˚W. Deep-Sea Res. I 52, 295-318.
Croot, P.L., Johanson M., 2000. Determination of iron speciation by cathodic stripping voltammetry in seawater using the competing ligand 2-(2-Thiazolylazo)-p-cresol (TAC). Electroanalysis 12, 565-576.
De Baar, H.J.W., Buma, A.G.J., Nolting, R.F., Cadée, G.C., Jacques, G., Tréguer, P.J., 1990. On iron limitation of the Southern Ocean: experimental observation in the Weddell and Scotia Seas. Mar. Ecol. Progr. Ser. 65, 105-122.
Ducklow, H.W., 2003. Seasonal production and bacterial utilization of DOC in the Ross Sea, Antarctica. Biogeochemistry of the Ross Sea, Antarctic Research Series, 78, 143-158.
Dulaquais, G., Waeles, M., Gerringa, L. J. A., Middag, R., Rijkenberg, M. J. A., Riso, R., 2018. The biogeochemistry of electroactive humic substances and its connection to iron chemistry in the North East Atlantic and the Western Mediterranean Sea. Journal of Geophysical Research: Oceans, 123. https://doi.org/10.1029/2018JC014211
Dunbar, R. B., Leventer, A. R., Mucciarone, D. A.,1998. Water column sediment fluxes in the Ross Sea, Antarctica: Atmospheric and sea ice forcing, J. Geophys. Res., 103, 30,741–30,759, doi:10.1029/1998JC900001.
Genovese, C., Grotti, M., Pittaluga,J., Ardini, F., Janssens, J., Wuttig, K., Moreau, S., Lannuzel, D.,2018. Influence of organic complexation on dissolved iron distribution in East Antarctic pack ice Mar. Chem. 203, 28–37 https://doi.org/10.1016/j.marchem.2018.04.005
Gerringa, L.J.A., Herman, P.M.J., Poortvliet, T.C.W., 1995. Comparison of the linear Van den Berg / Ružić transformation and a non-linear fit of the Langmuir isotherm applied to Cu speciation data in the estuarine environment. Mar. Chem. 48, 131-142.
Gerringa, L.J.A., Veldhuis, M.J.W. ,Timmermans, K.R.,Sarthou, G., de Baar, H.J.W, 2006. Co-variance of dissolved Fe-binding ligands with biological observations in the Canary Basin. Mar Chem., 102, 276-290. doi:10.1016/j.marchem.2006.05.004
Gerringa, L.J.A. Rijkenberg, M.J.A., Thuróczy, C-E, Maas, L.R.M., 2014. A critical look at the calculation of the binding characteristics and concentration of iron complexing ligands in seawater with suggested improvements. Environmental Chemistry, 11, 114-136.http://dx.doi.org/10.1071/EN13072
Gerringa, L.J.A., Laan, P., van Dijken, G.L., van Haren, H., De Baar, H.J.W., Arrigo, K.R., Alderkamp, A.-C., 2015a. Sources of iron in the Ross Sea polynya in early summer. Mar Chem. 177:447-459. .doi.org/10.1016/j.marchem.2015.06.002

Gerringa, L.J.A., Rijkenberg, M.J.A.,. Schoemann, V., Laan, P., de Baar, H.J.W.2015b. Organic complexation of iron in the West Atlantic Ocean. Mar Chem. 177:434-446. .doi.org/10.1016/j.marchem.2015.04.007

Gieskes, W.W.C., Engelkes, M.M., Kraay, G.W., 1991. Degradation of diatom chlorophyll to colorless, non-fluorescing compounds during copepod grazing. Hydrobiol. Bull. 25, 65–72.

Gledhill, M., Van den Berg, C.M.G., 1994. Determination of complexation of iron (III) with natural organic complexing ligands in seawater using cathodic stripping voltammetry. Mar. Chem. 47, 41-54.

Gledhill, M., Buck, K.N., 2012. The organic complexation of iron in the marine environment: a review. Frontiers in microbiology http://dx.doi.org/10.3389/fmicb.2012.00069.

Gledhill, M., Gerringa, L.J.A., Laan, P.,. Timmermans,K.R., 2015. Heme b quotas are low in Southern Ocean phytoplankton. MEPS, 532:29-40.

Gledhill M and Gerringa LJA , 2017. The Effect of Metal Concentration on the Parameters Derived from Complexometric Titrations of Trace Elements in Seawater—A Model Study. Front. Mar. Sci. 4:254. doi: 10.3389/fmars.2017.00254. P 1-15.

Gordon, A.L., Padman, L., Bergamasco, A., 2009. Southern Ocean shelf slope exchange. Deep-Sea Res. II Top. Stud. Oceanogr. 56, 775–777.

Grasshoff, K., Ehrhard, M., Kremling, K.,1983. Methods of seawater analysis. Weinheim: Verlag Chemie GmbH. 419 p.

Hansell, D.A., Carlson, C.A., Schlitzer, R., 2012. Net removal of major marine dissolved organic carbon fractions in the subsurface ocean. Glob. Biogeochem. Cycles 26, GB1016. http://dx.doi.org/10.1029/2011GB004069.

Hansell, D.A., Carlson, C.A., Repeta, D.J., Schlitzer, R., 2009. Dissolved organic matter in the ocean. A controversy stimulates new insights. Oceanography 22, 202–211.

Hassler, C.S., Schoemann, V., Nichols, C.M., Butler, E.C.V., Boyd, P.W., 2011.Saccharides enhance iron bioavailability to Southern Ocean phytoplankton. *Proc.Natl.Acad.Sci.U.S.A.* 108,1076–1081.doi:10.1073/pnas. 1010963108

Hassler, C.S., Van den Berg, C.M.G., Boyd, P.W., 2017. Toward a Regional Classification to Provide a More Inclusive Examination of the Ocean Biogeochemistry of Iron-Binding Ligands. Front. Mar. Sci. 4:19. doi: 10.3389/fmars.2017.00019

Hatta, M., Measures, C.I., Lam, P.J., Ohnemus, D.C., Auro, M.E., Grand, M.M., Selph, K.E., 2017. The relative roles of modified circumpolar deep water and benthic sources in supplying iron to the recurrent phytoplankton blooms above Pennell and Mawson Banks, Ross Sea, Antarctica. Journal of Marine Systems 166 (2017) 61–72. doi.org/10.1016/j.jmarsys.2016.07.009

Hawkes J.A., Connelly D.P., Gledhill, M., Achterberg, E.P., 2013. The stabilization and transportation of dissolved iron from high temperature hydrothermal vent systems. Earth Planet. Sci. Lett. 375, 280-290.

Hayes, D.E.; Davey, F.J., 1975. A Geophysical Study of the Ross Sea, Antarctica. Initial Reports of the Deep Sea Drilling Project, 28. Initial Reports of the Deep Sea Drilling Project. 28. doi:10.2973/dsdp.proc.28.134.1975.

Heller, M.I., Gaiero, D.M., Croot, P.L., 2013. Basin scale survey of marine humic fluorescence in the Atlantic: Relationship to iron solubility and H_2O_2. Global Biogeochem. Cycl., VOL. 27, 88–100, doi:10.1029/2012GB004427, 2013

Holm-Hansen, O., Lorenzen, C., Holmes, R.W., Strickland, J.D.H., 1965. Fluorometric determination of chlorophyll in Chlorophyta, Chrysophyta, Phaeophyta, Pyrrophyta. J Cons Perm Inter Explor Mer 30: 3–15.

Hudson, R.J.M., Covault, D.T., Morel, F.M.M., 1992. Investigations of iron coordination and redox reactions in seawater using 59Fe radiometry and ion-pair solvent extraction of amphiphilic iron complexes. Mar. Chem. 38, 209–235.

Hudson, R. J. M., Rue, E. L., Bruland, K. W., 2003. Modeling complexometric titrations of natural water samples. *Environ. Sci. Technol.*, *37*, 1553. doi:10.1021/ES025751A

Jacobs, S.S., Giulivi, C.F., 1999. Thermohaline Data and Ocean Circulation on the Ross Sea Continental Shelf. In: Spezie, G., Manzella, G.M.R. (Eds.), Oceanography of the Ross Sea Antarctica, pp. 3–16.

Johnson, K.S., et al., 2007. Developing standards for dissolved iron in seawater. EOS Trans.Am. Geophys. Union 88 (11), 131–132.

Kitayama, S., Kuma, K. Manabe, E. Sugie, K. Takata, H. Isoda, Y. Toya, K. Saitoh, S.-i. Takagi, S. Kamei Y., Sakaoka, K. (2009). Controls on iron distributions in the deep water column of the North Pacific Ocean: Iron(III) hydroxide solubility and marine humic-type dissolved organic matter J. Geophys. Res., 114, C08019, doi:10.1029/2008JC004754.

Klunder MB, Laan P, Middag R, De Baar HJW, van Ooijen JC (2011) Dissolved iron in the Southern Ocean (Atlantic sector). Deep Sea Res II 58:2678–2694.

Kustka, A.B., Kohut, J.T., White, A.E., Lam, P.J., Milligan, A.J., Dinniman, M.S., Mack, S., Hunter, E., Hiscock, M.R., Smith Jr, W.O., Measures C. I., 2015a. The roles of MCDW and deep water iron supply in sustaining a recurrent phytoplankton bloom on central Pennell Bank(RossSea). Deep-Sea ResearchI105(2015)171–185. doi.org/10.1016/j.dsr.2015.08.012

Kustka, A.B., Jones, B.M., Hatta, M., Field, M.P., Milligan, A.J., 2015b.The influence of iron and siderophores on eukaryotic phytoplankton growth rates and community composition in the Ross Sea. Marine Chemistry 173 (2015) 195–207. doi.org/10.1016/j.marchem.2014.12.002

Laglera, L.M., Battaglia, G., Van den Berg, C.M.G., 2007. Determination of humic substances in natural waters by cathodic stripping voltammetry of their complexes with iron. *Anal.Chim.Acta* 599,58–66. doi:10.1016/j.aca.2007.07.059

Laglera, L.M., Battaglia, G., Van den Berg, C.M.G., 2011. Effect of humic substances on the iron speciation in natural waters by CLE/CSV. Mar. Chem. 127, 134–143.

Laglera, L.M., Tovar-Sánchez, A., Iversen, M.H., González, H.E., Naik, H., Mangesh, G., Assmy, P., Klaas, C., Mazzocchi, M.G., Montresor, M., Naqvi, S.W.A., Smetacek, V.,Wolf-Gladrow, D.A., 2017. Iron partitioning during LOHAFEX: Copepod grazing as a major driver for iron recycling in the Southern Ocean Mar. Chem.196, 148–161. http://dx.doi.org/10.1016/j.marchem.2017.08.011

Laglera, L.M., Tovar-Sánchez, A., Sukekava, C.F., Naik, H., , Naqvi, S.W.A., Wolf-Gladrow, D.A., 2019. Iron organic speciation during the LOHAFEX experiment: Iron ligands release under biomass control by copepod grazing. Journal of Marine Systems in press. doi.org/10.1016/j.jmarsys.2019.02.002

Lannuzel, D., Schoemann, V., de Jong, J.T.M., Chou, L., Delille, B., Becquevort, S., Tison, J.L., 2008. Iron study during a time series in the western Weddell pack ice. Mar. Chem. 108, 85–95.

Lannuzel, D., Grotti, M., Abelmoschi, M.L., van der Merwe, P., 2015. Organic ligands control the concentration of DFe in Antarctic Sea ice. Mar. Chem. 174, 120–130. http://dx.doi.org/10.1016/j.marchem.2015.05.005

Liu, X., Millero, F.J., 2002. The solubility of iron in seawater. Mar.Chem. 77, 43-54.

Marsay, C.M., Sedwick, P.N., Dinniman, M.S., Barrett, P.M., Mack, S.L., McGillicuddy, D.J., 2014. Estimating the benthic efflux of dissolved iron on the Ross Sea continental shelf. Geophys Res. Lett., 41, 7576–7583, doi:10.1002/2014GL061684.

Martin, J.H., Fitzwater, S.E., Gordon, R.M., 1990. Iron deficiency limits phytoplankton growth in Antarctic waters. Glob. Biogeochem. Cyc. 4, 5-12.

Martin, J.H., Coale, K.H., Johnson, K.S., Fitzwater, S.E. Gordon, R.M., Tanner, S.J., Hunter, C.N., Elrod, V.A., Nowicki, J.L., Coley, T.L., Barber, R.T., Lindley, S., Watson, A.J., van Scoy, K., Law, C.S., Liddicoat, M.I., Ling, R., Station, T., Stockel, J., Collins, C., Anderson, A., Bidigare, R., Ondrusek, M., Latasa, M., Millero, F.J., Lee, K., Yao, W., Zhang, J.Z., Friederich, G., Sakamoto, C., Chavez, F., Buck, K., Kolber, Z., Green, R., Falkowski, P., Chisholm, S.W., Hoge, F., Swift, R., Yangel, J., Turner, S., Nightingale, P., Hatton, A., Liss, P., Tindale, N.W., 1994. Testing the iron hypothesis in ecosystems of the equatorial Pacific Ocean. Nature 371, 123-129.

Mawji, E., Gledhill, M., Milton, J.A., Zubkov, M. V, Thompson, A., Wolff, G.A., Achterberg, E.P., 2011. Production of siderophore type chelates in Atlantic Ocean waters enriched with different carbon and nitrogen sources. Mar. Chem. 124, 90–99.

McGillicuddy, D. J., Jr., Sedwick, P.N., Dinniman, M.S., Arrigo, K.R., Bibby, T. S., Greenan, B. J. W., Hofmann, E. E., Klinck, J. M., Smith Jr., W. O., Mack, S. L., Marsay, C. M., Sohst, B. M., van Dijken, G. L., 2015. Iron supply and demand in an Antarctic shelf ecosystem, Geophys. Res. Lett.,42, 8088–8097, doi:10.1002/2015GL065727

Millero, F.J., 1998. Solubility of Fe(III) in seawater. Earth Planet. Sci. Lett. 154, 323–330.

Murphy, J. & Riley, J.P., 1962. A modified single solution method for the determination of phosphate in natural waters. Analytica chim. Acta 27, 31-36.

Nakayama, Y., S. Fujita, K. Kuma, and K. Shimada (2011), Iron and humic-type fluorescent dissolved organic matter in the Chukchi Sea and Canada Basin of the western Arctic Ocean, J. Geophys. Res., 116, C07031, doi:10.1029/2010JC006779.

Nelson, N.B., Siegel, D.A., 2013.The Global Distribution and Dynamics of Chromophoric Dissolved Organic Matter Annu. Rev. Mar. Sci. 2013. 5:447–7610.1146/annurev-marine-120710-100751.

Orsi, A.H., Wiederwohl, C.L., 2009. A recount of Ross Sea waters. Deep-Sea Res. II 56, 778–795 .

Poorvin, L., Sander, S.G., Velasquez, I., Ibisanmi, E., LeCleir, G.R., Wilhelm, S.W., 2011. A comparison of Fe bioavailability and binding of a catecholate siderophore with virus-mediated lysates from the marine bacterium Vibrio alginolyticus PWH3a. J. Exp. Mar. Bio. Ecol. 399, 43–47.

Repeta, D.J., Aluwihare, L.I., 2006. High molecular weight dissolved organic carbon cycling as determined by radiocarbon measurements of neutral sugars. *Limnology and Oceanography* 51:1,045–1,053.

Rivaro, P., Ardini,F., Grotti,M.,Aulicino,G., Cotroneo,Y., Fusco, G., Mangoni,O., Bolinesi,F., Saggiomo,M., Celussi, M.,2018. Mesoscale variability of iron speciation in a coastal Ross Sea area (Antarctica) during summer 2014. Geology and Ecology,https://doi.org/10.1080/02757540.2018.1531987

Rue, E.L., Bruland, K.W., 1995. Complexation of iron(II1) by natural organic ligands in the Central North Pacific as determined by a new competitive ligand equilibration/adsorptive cathodic stripping voltammetric method. Mar. Chem. 50, 117–138.

Rijkenberg, M.J.A., Gerringa, L.J.A., Carolus, V.E., Velzeboer, I.,de Baar, H.J.W., 2006. Enhancement and inhibition of iron photoreduction by individual ligands in open ocean seawater. Geochim, Cosmochim Acta, 70, 2790-2805. doi:10.1016/j.gca.2006.03.004

Rijkenberg, M.J.A., Gerringa, L.J.A., Timmermans, K.R.,. Fischer, A.C.,. Kroon, K.J., Buma, A.G.J., Wolterbeek, H.Th., de Baar, H.J.W.,2008. Enhancement of the reactive iron pool by marine diatoms. Mar Chem. 109, 29-44. doi:10.1016/j.marchem.2007.12.001

Ryan-Keogh, T.J., DeLizo, L.M., Smith Jr., W.O., Sedwick, P.N., McGillicuddy Jr., D.J., Moore, C.M., Bibby, T.S., 2017. Temporal progression of photosynthetic-strategy in phytoplanktonin the Ross Sea, Antarctica. J. Mar. Syst. 166, 87–96.

Sander, S.G., Koschinsky, A., 2011. Metal flux from hydrothermal vents increased by organic complexation. Nat. Geosci. 4, 145–150.

Sarthou, G., Vincent, D., Christaki, U., Obernosterer, I., Timmermans, K.R., Brussaard, C.P.D., 2008. The fate of biogenic iron during a phytoplankton bloom induced by natural fertilization: impact of copepod grazing. Deep-Sea Res. II 55, 734-751.

Schlitzer, R., Ocean Data View, https://odv.awi.de, 2018.

Sedwick, P. N., DiTullio, G. R., Mackey, D. J., 2000. Iron and manganese in the Ross Sea, Antarctica: Seasonal iron limitation in Antarctic shelf waters, J. Geophys. Res., 105, 11,321– 11,336, 2000

Sedwick, P.N., Marsay, C.M., Sohst, B.M., Aguilar-Islas, A.M., Lohan,M.C., Long, M.C., Arrigo, K.R., Dunbar, R.B., Saito,M.A., Smith,W.O., Di Tullio, G.R., 2011. Early season depletion of dissolved iron in the Ross Sea polynya: implications for iron dynamics on the Antarctic continental shelf. J. Geophys. Res. 116, C12019.

Sherrell, R.M., Lagerström, M.E., Forsch, K.O., Stammerjohn, S.E., Yager, P.L., 2015 Dynamics of dissolved iron and other bioactive trace metals (Mn, Ni, Cu, Zn) in the Amundsen Sea Polynya, Antarctica. Elementa: Science of the Anthropocene • 3: 000071 • doi: 10.12952/journal.elementa.000071

Slagter, H.A., Gerringa, L.J.A., Brussaard, C.P.D., 2016. Phytoplankton virus production negatively affected by iron limitation. Front. Mar. Sci. 3:156. doi: 10.3389/fmars.2016.00156

Slagter, H.A., Reader, H,.E., Rijkenberg, M.J.A., Rutgers van der Loeff, M., de Baar, H.J.W., Gerringa, L.J.A.,2017. Fe speciation is related to terrestrial dissolved organic matter in the Arctic Ocean. Marine Chemistry 197 (2017) 11–25. http://dx.doi.org/10.1016/j.marchem.2017.10.005

Slagter, H.A., Laglera, L.M., Sukekava, C., Gerringa, L.J.A. 2019. Fe-binding organic ligands in the humic-rich TransPolar Drift in the surface Arctic Ocean using multiple voltammetric methods. *Journal of Geophysical Research: Oceans*, . DOI: 10.1029/2018JC014576

Smith, W.O., Barber, D.G., eds., 2007. Polynyas: Windows to the World. Elsevier Oceanography Series, vol. 74, Elsevier, Amsterdam.

Smith Jr., W.O., Ainley, D.G., Arrigo, K.R., Dinniman, M.S., 2014. The oceanography and ecology of the Ross Sea. Ann. Rev. Mar. Sci. 6, 469–487.

Smith Jr., W.O., Dinniman, M.S., Klinck, J.M., Hoffman, E.,2003. Biogeochemical climatologies in the Ross Sea, Antarctica: seasonal patterns of nutrients and biomass. Deep-Sea Research II 50, 3083–3101.

Smith, W.O., Shields, A.R., Peloquin, J.A., Catalano, G., Tozzi, S., Dinniman, M.S., Asper, V.A., 2006. Interannual variations in nutrients, net community production, and biogeochemical cycles in the Ross Sea. Deep-Sea Res. II, 53, 815–833.

SooHoo, J.B., Kiefer, D.A., 1982. Vertical distribution of phaeopigments_ l. A simple grazing and photo oxidative scheme for small particles. Deep-Sea Research, Vol. 29, No. 12A, pp. 1539 to 1551.

Strickland, J.D.H. and Parsons, T.R., 1968. A practical handbook of seawater analysis. first edition, Fisheries Research Board of Canada, Bulletin. No 167, 1968. p.65.

Strzepek, R.F., Maldonado, M.T., Hunter, K.A., Frew, R.D., Boyd, P.W., 2011. Adaptive strategies by Southern Ocean phytoplankton to lessen iron limitation: Uptake of organically complexed iron and reduced cellular iron requirements Limnol. Oceanogr. 56, 1983-2002.

Sunda, W.G., Huntsman, S.A., 1997. Interrelated influence of iron, light and cell size on marine phytoplankton growth. Nature 390, 389-392.

Tagliabue, A., Bopp, L., Dutay, J.-C., Bowie, A.R., Chever, F., Jean-Baptiste,.P., Bucciarelli, E., Lannuzel, D., Remenyi, T., Sarthou, G., Aumont, O., Gehlen, M., Jeandel, C., 2010. Hydrothermal contribution to the oceanic dissolved iron inventory. Nature Geosci. 14, 1-5, doi:10.1038/NGEO818.

Tagliabue, A., and K. R. Arrigo. 2003. Anomalously low zooplankton abundance in the Ross Sea: An alternative explanation. Limnology and Oceanography, 48, 686-699

Tani, H., Nishioka,J.,. Kuma, K.,Takata, H., Yamashita, Y., Tanoue E., Midorikawa, T., 2003. "Iron(III) hydroxide solubility and humic-type fluorescent organic matter in the deep water column of the Okhotsk Sea and the northwestern North Pacific Ocean. DSR-I, 50: 1063-1078.

Thuróczy, C.-E., Gerringa, L., Klunder, M., Laan, P., De Baar, H., 2011. Observation of consistent trends in the organic complexation of dissolved iron in the Atlantic sector of the Southern Ocean. Deep-Sea Res. II 58, 2695-2706.

Thuróczy, C-E, Alderkamp, A.-C., Laan, P, Gerringa, L.J.A., De Baar H.J.W., Arrigo, K.R., 2012. Key role of organic complexation of iron in sustaining phytoplankton blooms in the Pine Island and Amundsen Polynyas (Southern Ocean). Deep-Sea Res. II 71-76, 49-60.

Timmermans, K. R., Gerringa, L. J. A., de Baar, H. J. W., van der Wagt, B., Veldhuis, M. J. W., de Jong, J.T.M., Croot, P. L., Boye, M., 2001. Growth rates of large and small Southern Ocean diatoms in relation to availability of iron in natural seawater, Limnol. Oceanogr., 46, 260–266, doi:10.4319/lo.2001.46.2.0260.

Tomczak, M., Godfrey, J.S., 2001. Regional Oceanography: an Introduction. Elsevier, Oxford.

Velasquez, I., Ibisanmi, E., Maas, E.W., Boyd, P.W., Nodder, S., Sander, S. G., 2016. Ferrioxamine siderophores detected amongst iron binding ligands produced during the remineralization of marine particles. *Front.Mar.Sci.* 3:172.doi:10.3389/fmars.2016.00172

Visser, F., L.J.A. Gerringa, S.J. van der Gaast, H.J.W de Baar and K.R. Timmermans, 2003. The role of reactivity and iron content of aerosol dust on growth rates of two Antarctic diatom species. J. Phycol. 39 (6): 1085-1094.

Watanabe, K., Fukuzaki, K., Fukushima, K.,. Aimoto, M., Yoshioka, T., Yamashita,Y., 2018. Iron and fluorescent dissolved organic matter in an estuarine and coastal system in Japan. Limnology 19 : 229–240